Journal of Colloid and Interface Science 421 (2014) 132–140

Contents lists available at ScienceDirect

Journal of Colloid and Interface Science

www.elsevier.com/locate/jcis

Layer-by-layer assembly of polymersomes and polyelectrolytes on planar surfaces and microsized colloidal particles

Marcos Coustet [a], Joseba Irigoyen [b], Teodoro Alonso Garcia [b], Richard A. Murray [b], Gabriela Romero [b], M. Susana Cortizo [a], Wolfgang Knoll [c], Omar Azzaroni [a,*], Sergio E. Moya [b,*]

[a] Instituto de Investigaciones Fisicoquímicas Teóricas y Aplicadas (INIFTA), Departamento de Química, Facultad de Ciencias Exactas, Universidad Nacional de La Plata (UNLP), CONICET, Diagonal 113 y 64 (1900), La Plata, Argentina
[b] CIC BiomaGUNE, 182 Paseo Miramón, 20009 San Sebastián, Spain
[c] Austrian Institute of Technology (AIT), Donau-City-Strasse 1, 1220 Vienna, Austria

ARTICLE INFO

Article history:
Received 2 December 2013
Accepted 29 January 2014
Available online 4 February 2014

Keywords:
Layer-by-layer assembly
Colloidal nanomaterials
Polymersomes

ABSTRACT

Hybrid polyelectrolyte multilayer systems were fabricated on top of planar surfaces and colloidal particles via layer by layer (LbL) assembly of polystyrene sulphonate (PSS) and polybenzyl methacrylate-*block*-poly(dimethylamino)ethyl methacrylate (PBzMA-*b*-PDMAEMA) polymersomes. Polymersomes were prepared by self assembly of PBzMA-*b*-PDMAEMA copolymer, synthesised by group transfer polymerisation. Polymersomes display a diameter of 270 nm and a shell thickness of 11 nm. Assembly on planar surfaces was followed by means of the Quartz Crystal Microbalance with Dissipation (QCM-D) and Atomic Force Microscopy (AFM). Detailed information on the assembly mechanism and surface topology of the polymersome/polyelectrolyte films was thereby obtained. The assembly of polymersomes and PSS on top of silica particles of 500 nm in diameter was confirmed by ζ-potential measurements. Confocal laser scanning microscopy (CLSM), scanning electron microscopy (SEM) and transmission electron microscopy (TEM) revealed that polymersome/PSS coated silica particles increase in total diameter up to 3–5 μm. This hints toward the formation of densely packed polymersome layers. In addition, CLSM showed that polymersome/PSS films exhibit a high loading capacity that could potentially be used for encapsulation and delivery of diverse chemical species. These results provide an insight into the formation of multilayered films with compartmentalised hydrophilic/hydrophobic domains and may lead to the successful application of polymersomes in surface-engineered colloidal systems.

1. Introduction

The tunable construction of thin-film-based nanoarchitectures via layer-by-layer (LbL) assembly has opened up new horizons in materials science and led to exciting new developments in many scientific areas during the past two decades [1–4]. One major advantage of LbL assembly is the intrinsic potential for the combination of diverse building blocks through complementary interactions, i.e.: electrostatic interactions, hydrogen bonding, etc., to create thin films displaying functional groups and chemical entities at controlled sites in nanoscale arrangements. From the standpoint of methodology, the LbL toolbox [5] is currently able to offer a broad spectrum of nanocomposite thin films [6] compatible with multiple applications i.e.: drug delivery, antifouling coatings, nanodevices, membranes for nanofiltration, etc. [7–12].

Initially, LbL assembly was developed to produce nanoscale films through the alternate deposition of oppositely charged polyelectrolytes [13]. Thereafter, the LbL method was successfully extended to other building blocks. A broad variety of multilayer composite films have been constructed by replacing one or both polyelectrolyte counterparts with other charged building blocks such as proteins [14], dendrimers [15], lipids [16] and colloidal nanoparticles [17]. In this regard, LbL assemblies fabricated upon micelles [18,19] or vesicles [20] have proven to be very efficient in confining and hosting different chemical species within the LbL film. The use of "soft" nanocapsules to promote the selective loading of predefined host molecules into LbL thin films represents a research topic of growing relevance in supramolecular materials science [21,22]. For example, Zhang and co-workers have proposed the use of block copolymer micelles as matrices for the

* Corresponding authors.
E-mail addresses: azzaroni@inifta.unlp.edu.ar (O. Azzaroni), smoya@cicbiomagune.es (S.E. Moya).
URLs: http://softmatter.quimica.unlp.edu.ar (O. Azzaroni), http://www.cicbiomagune.com (S.E. Moya).

http://dx.doi.org/10.1016/j.jcis.2014.01.038
0021-9797/

incorporation of organic species and the fabrication of LbL films by the alternate deposition of the block copolymer micelles and polyelectrolytes [23].

In a similar vein the integration of lipid vesicles [24] into polyelectrolyte multilayers has also shown great versatility to enhance the loading capacity of the multilayers for potential drug delivery applications. However, lipid vesicles have very poor stability and easily rupture when interacting with polyelectrolytes during LbL assembly [25]. Within this framework we should emphasise that the incorporation of polymer vesicles in LbL assemblies remains almost completely unexplored [26]. Polymeric vesicles, also known as "polymersomes", are hollow, lamellar spherical structures (self-assembled polymer shells) composed of block copolymer amphiphiles [27,28]. Hydrophobic blocks of each copolymer aggregate and minimise direct exposure to water whilst hydrophilic blocks form inner and outer hydrophilic layers in contact with aqueous media, thus resembling a typical bilayer vesicle formed by lipids [29]. However, compared with lipids, the larger molecular weight and restricted conformational freedom of block copolymer polymer chains endow polymersomes with enhanced durability and reduced water permeability [30]. In recent years polymersomes have received considerable attention within the materials science community due to their improved mechanical properties, high stability, and ability to incorporate compounds not only in the aqueous core but also in the hydrophobic domains [31,32].

In this context, polymersomes may result in interesting building blocks to create LbL assemblies exhibiting high loading capabilities. Such assemblies could be applied for oil, perfume, dye encapsulation in surface coatings as well as for drug delivery, especially in topical applications where there may be safety concerns related to the chemistry of the polymers. A thorough understanding of multilayer formation with polymersomes is essential for exploring new classes of materials to engineer LbL assemblies. Therefore, this work aims at providing a deeper insight into the self assembly of polymersomes with polyelectrolytes in LbL films. As building blocks for the films we have chosen polymersomes fabricated upon polybenzyl methacrylate-*block*-poly(dimethylamino)ethyl methacrylate block copolymer, which is positively charged, and polystyrene sulphonate, a negatively charged polyelectrolyte. Since polymersomes are themselves self assembled particles the films fabricated on the basis of alternating polymersomes and polyelectrolyte deposition will have a higher degree of organisation than standard LbL films.

We first explored the mechanism of assembly of polymersomes with the Quartz Crystal Microbalance with Dissipation (QCM-D) and Atomic Force Microscopy (AFM). Polymersomes are quite large structures in comparison with the counter polyelectrolytes. Because of this feature we observed that the coating of planar surfaces by LbL assembly of polymersomes and polyelectrolytes resulted in a discontinuous arrangement of polymersomes. However, a completely different situation was observed when the LbL process is performed on top of colloidal particles, where the polymersomes form large shells around the support colloidal particle after 4 assembly steps. We observed that the assemblies are indeed significantly larger than the particles on top of which of the coating was grown. The difference in the structures produced by the assembly of polymersomes on top of planar and spherical surfaces are explained on the basis of the differences in the assembly protocols. In particular, the use of centrifugation during the coating of the colloidal particles generates a high concentration of polymersomes around the silica particles that are responsible for the formation of the thick polymer shell. The large polymersome assemblies produced on top of silica particles could have applications in encapsulation and drug delivery. ζ potential measurements, Confocal Laser Scanning Microscopy (CLSM), Scanning Electron Microscopy (SEM) and Transmission Electron Microscopy (TEM) were used to characterise the LbL assembly on colloidal particles.

2. Experimental

2.1. Chemicals and reagents

Poly(allylamine hydrochloride) (PAH) ($M_w \sim 15{,}000$), poly(sodium 4-styrenesulphonate) (PSS) ($M_w \sim 70{,}000$), benzyl methacrylate (BzMA, 96%), 2-(dimethylamino)ethyl methacrylate (DMAEMA, 98%) monomers, the initiator, 1-methoxy-1-trimethylsiloxy-2-methyl propene (MTS), tetrabutylammonium hydroxide and benzoic acid, polystyrene sulphonate (PSS) (M_w 70,000), NaCl, rhodamine B were all purchased from Sigma–Aldrich. Monomers were purified by vacuum distillation and stored in the presence of activated 4A molecular sieves before use. Chloroform (Carlo Erba, 99%) for HPLC was used as purchased. Tetrahydrofuran (THF, Carlo Erba, 99.8%), the polymerisation solvent, was refluxed under nitrogen over sodium (Na)/benzophenone (BP) in a controlled atmosphere still until blue colour of medium. The THF was then distilled into a flask with activated 4A molecular sieves and stopped with septum stopcock. The polymerisation catalyst, tetrabutylammonium bibenzoate (TBABB), was prepared from the reaction of tetrabutylammonium hydroxide with benzoic acid according to Dicker et al. [33] and was kept under vacuum until use.

2.2. Block copolymer synthesis and characterisation

Diblock copolymer of benzyl methacrylate (BzMA) and 2-(dimethylamino)ethyl methacrylate (DMAEMA) units, was prepared by group transfer polymerization [34,35] (GTP) in THF using glass reactor under dry nitrogen and standard Schlenk techniques as described elsewhere [36]. The chemical structure was determined by ^{1}H NMR employing a Varian-200 MHz (Mercury 200) at 35 °C in $CDCl_3$. Tetramethylsilane (TMS) was used as an internal standard. δ(ppm): 1.06–0.73 (–C**H**$_3$, m, 6H); 1.91–1.79 (–C**H**$_2$–, m, 4H); 2.28 (–N(C**H**$_3$)$_2$, s, 6H); 2.56 (–C**H**$_2$–N<, t, 2H); 4.06 (–O–C**H**$_2$–, t, 2H); 4.90 (Ar–C**H**$_2$–, s, 2H); 7.28 (Ar**H**, m, 5H). The molecular weight distribution and average molecular weights were determined by size exclusion chromatography (SEC), using a LKB-2249 instrument at 25 °C. A series of four μ-Styragel® columns with pore sizes of 10^5, 10^4, 10^3, 100 Å, was used with chloroform as an eluent. The sample concentration was 4–5 mg/ml and the flow rate was 0.5 ml/min. The polymer was detected by a Shimadzu (SPD-10A) UV/VIS detector at 254 nm. The calibration was done with polystyrene standards supplied by Polymer Laboratories and Polysciences, Inc. The resulting number-average molecular weight (M_n) is 2.6 kDa and 4.5 kDa for the first block (PBzMA homopolymer) and the final copolymer, respectively. A dispersity, (D) = M_w/M_n, where M_w is the weight-average molecular weight, of 1.2 for both, homo and block copolymer was determined by SEC, which agrees with the expected values for this type of polymerisation [26]. The ratio of the two blocks in the copolymer (56:44), was estimated from the integral ratio of the peaks of aromatic and methylene hydrogen at 7.28 and 4.06 ppm, respectively, from the ^{1}H NMR spectrum. The critical micelle concentration (CMC) of poly(benzyl methacrylate)-*block*-poly(2-(dimethylamino)ethyl methacrylate) copolymers as measured by fluorescence spectroscopy and conductivity was found to be in the 10^{-4} to 10^{-3} M range.

2.3. ζ Potential

The ζ-potential of polymersomes and of the SiO_2 particles after each polymersome and PSS assembly were measured with a Malvern NanoSizer (Nano-ZS) (UK). All the ζ-potential measurements

were performed at 25 °C and with a cell drive voltage of 30 V, using a monomodal analysis model. Polymersomes measurements were performed at pH 2 (unless otherwise indicated) with varying NaCl concentration (10–200 mM).

2.4. Quartz Crystal Microbalance with Dissipation (QCM-D)

The alternating assembly of polymersomes and PSS on planar substrates was followed with a QCM-D E4, from Q-sense. The assembly was performed on silica coated quartz crystals with a 5 MHz resonance, also from Q-Sense.

2.5. Atomic Force Microscopy (AFM)

AFM images were taken with a Veeco Multimode AFM connected to a Nanoscope V controller, and imaged in tapping mode in a closed fluid cell filled with 10 mM NaCl solution. The particular silicon nitride cantilever used was a DNP-S10 available from Bruker with $K = 0.32\ \mathrm{Nm^{-1}}$. Substrates used were silica coated quartz crystals on top of which polyelectrolyte-polymersome bilayers were deposited.

2.6. Scanning Electron Microscopy (SEM)

SEM images were taken with a JEOL 6490LV microscope. Samples were deposited and dried onto carbon coated 400 square mesh copper TEM grids at room temperature and later metallised with a gold–palladium layer.

2.7. Transmission Electron Microscopy (TEM)

Ultra high resolution TEM was performed with a JEOL JEM 2100F microscope. Polymersomes were negatively stained with uranyl acetate (the grid was previously glow discharged) while silica colloids coated with $(PBzMA\text{-}b\text{-}PDMAEMA)_4/(PSS)_4$ multilayers were negatively stained with ammonium molybdate (the grid was previously glow discharged and treated with a solution of $MgCl_2$ 40 mM and $CaCl_2$ 40 mM).

2.8. Confocal Laser Scanning Microscopy (CLSM)

Images were taken on a Carl Zeiss LSM 510 inverted confocal microscope system, using a C-Apochromat 40x/1.20 W Korr UV–VIS-IR M27 objective and 488 nm excitation. Samples were mounted on standard microscope slides available from Menzel-Gläser.

2.9. Layer by layer assembly (LbL)

The fabrication of polymersome/PSS multilayer thin films was carried out as follows. Cleaned silicon substrates were first coated with 3 PAH/PSS bilayers by exposing them alternately to 1 mg/mL solutions of the corresponding polyelectrolytes in 0.1 M NaCl followed by extensive washing with water. Subsequently, the substrate was dipped into the cationic solution of PBzMA-*b*-PDMAEMA polymersomes in 0.1 M NaCl. Aqueous solutions were adjusted to pH = 2 with 0.1 M HCl. The two-step process was repeated several times in order to generate a multilayer of polymersomes and polyelectrolytes. Because of the thorough rinsing and the ready solubility of the polymer vesicles and PSS, this procedure ensures that only the electrostatically interacting building blocks remain on the surface. Typical adsorption times were 15–20 min per layer. The surface of the films was extensively rinsed after adsorption of each layer.

LbL modification of microsised silica particles was accomplished by following the general methods reported elsewhere [37]. Briefly, a solution of polymersomes was added to an aqueous dispersion of silica particles and were allowed to adsorb on the particles for 20 min with continual stirring. The dispersion was rinsed by three centrifugation/supernatant exchange/water redispersion cycles to remove excess polymer. PSS (1 mg/mL in 0.1 M NaCl) was subsequently adsorbed onto the polymersome-coated particles using the same procedure. The entire process was repeated several times in order to produce a four-bilayer polymersome/PSS film on the silica particles.

3. Results and discussion

Polymer vesicles were prepared by the so-called solvent-switch technique [38] using polybenzyl methacrylate-*block*-poly(dimethylamino)ethyl methacrylate copolymer (2.6–1.9 kDa) as the constituting building blocks. The amphiphilic copolymer was dissolved in DMF and then, water is added gradually to the copolymer solution. This process led to the association of the hydrophobic blocks in the polar environment to form a vesicle membrane whereas the hydrophilic blocks are solvated to form the vesicle corona which colloidally stabilises the vesicle. The *z* average diameter of the as-synthesised polymersomes was 275 nm with a narrow distribution (Fig. 1a). Results obtained from light scattering measurements were also corroborated by scanning electron microscopy Fig. 1b shows a SEM image of PBzMA-*b*-PDMAEMA polymersomes deposited on a silicon wafer in which the narrow size distribution is clearly observed. Polymersomes were also characterised by TEM imaging revealing the presence of unilamellar structures. The

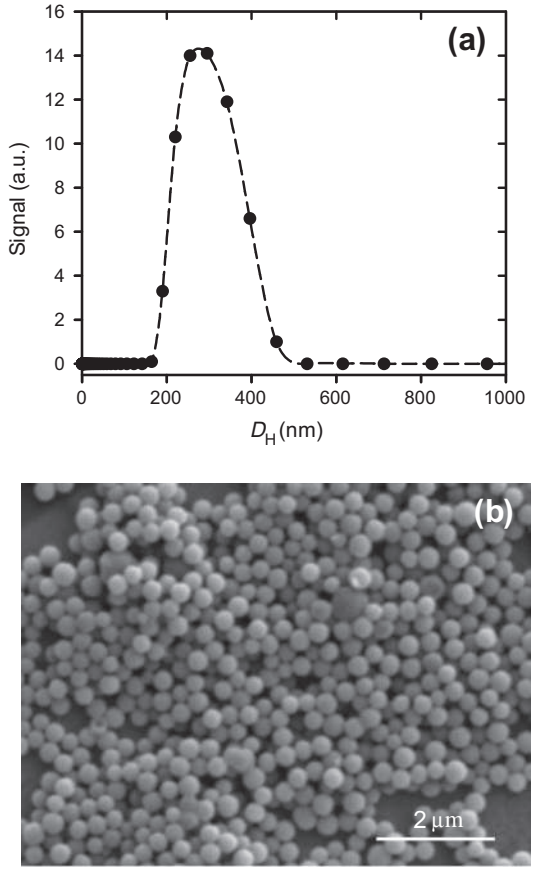

Fig. 1. (a) Size distribution of PBzMA-*b*-PDMAEMA polymersomes as obtained by Dynamic Light Scattering. (b) SEM images of PBzMA-*b*-PDMAEMA polymersomes obtained by the solvent-switch technique.

thickness of the polymer wall was close to 11 nm, as estimated from TEM characterisation (Fig. 2).

The ζ potential of PBzMA-*b*-PDMAEMA vesicles in 0.1 M KCl solution (pH = 6) was +52 mV. The effective charge of the polymersomes under different experimental conditions represents a crucial parameter in the LbL technique provided that electrostatic interactions are the main driving force governing the assembly process. In this context we measured the ζ potential of PBzMA-*b*-PDMAEMA vesicles at different pH values and salt concentrations. Rehfeldt et al. [39] showed that the degree of protonation of PDMAEMA at pH 5 is about 85%, at pH 7 around 23%, and at pH 8 ca. 13%. Fig. 3a shows that the ζ potentials of polymersomes at pH 2, 6 and 10 correspond to +36.5, +36.5 and +23.8 mV, respectively. Measurements performed on vesicles under different electrolyte concentrations (Fig. 3b) and at a constant proton concentration (pH = 5) revealed that the ζ potential varies from +57 to +46 mV with varying KCl concentration (10–200 mM). This implies that polymersomes behave as cationic building blocks over a wide range of experimental conditions, i.e.: pH and ionic strength.

The assembly of the PBzMA-*b*-PDMAEMA polymersome/PSS and PSS on top of planar surfaces (Fig. 4) was first monitored by means of QCM-D. The systematic decrease in frequency as the substrate is alternatively brought into contact with the solutions of PBzMA-*b*-PDMAEMA vesicles and PSS demonstrates a regular and continuous film buildup as can be observed in Fig. 5. In fact, the mass of PBzMA-*b*-PDMAEMA/PSS multilayers constructed by the LbL strategy increases linearly with the number of deposition steps.

PBzMA-*b*-PDMAEMA polymersomes are positively charged and rapidly assemble on top of the PSS layer. However, a sharp increase in frequency after rinsing reveals that a significant fraction of the vesicles are loosely bound to the PSS layer and are easily removed from the surface after the rinsing step. This is not the case for PSS layers which remain firmly attached, even after extensive rinsing. Fig. 5 shows that the frequency shift decreases and the dissipation increases during vesicle injection while the opposite evolution is observed during the rinsing step. Each polymersome deposition stage leads to a dissipation increase of the same magnitude. Dissipation drops off when PSS is assembled but it can also be observed that there is a progressive increase in dissipation as the number of layers increases. The hydrophilic blocks of the PBzMA-*b*-PDMAEMA protruding out of the polymersomes are likely to be responsible for the high dissipation after polymersome deposition. This explanation is plausible considering that these blocks can be regarded as polymer brushes that confer a strong viscoelastic character to the system [40,41]. The deposition of PSS on top of the assembly and most likely in between the PDMAEMA chains must restrict the conformational freedom of these chains as they are "crosslinked" by the PSS [42]. The increase in the dissipation with the number of assembled PSS layers is probably due to the increase in roughness of the films as the number of assembled polymersome and PSS layers increases due to incomplete coating of the surface as corroborated by AFM (see below).

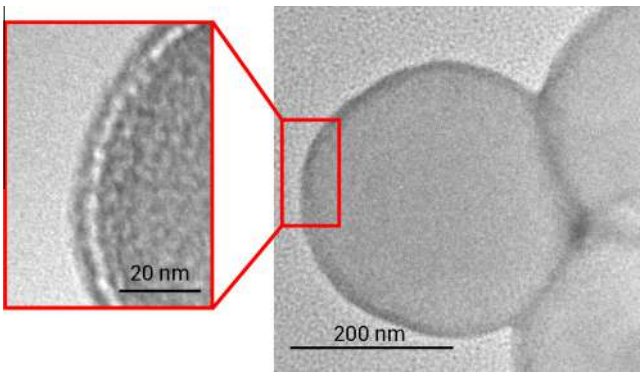

Fig. 2. TEM image of a PBzMA-*b*-PDMAEMA polymersome. The polymersome was stained with uranyl acetate The inset figure shows a portion of the polymersome at a higher magnification.

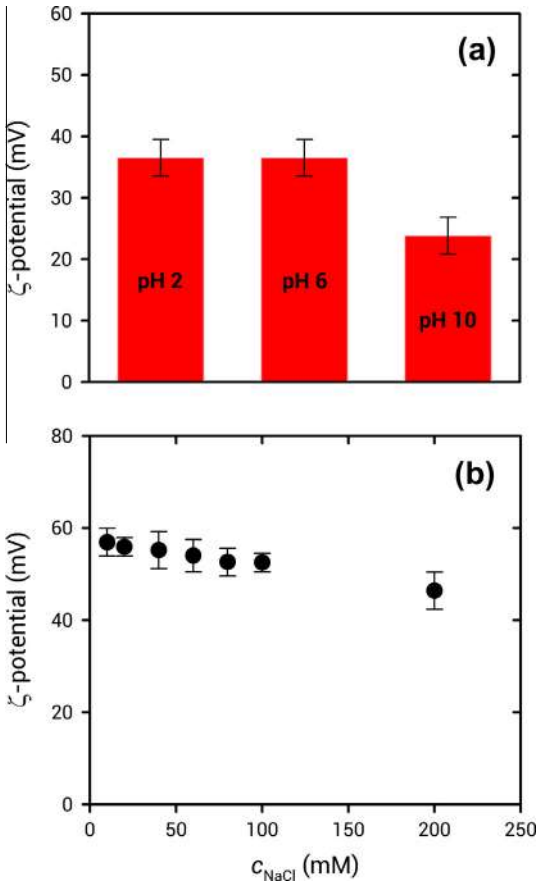

Fig. 3. ζ Potential of PBzMA-*b*-PDMAEMA vesicles as a function of (a) pH and (b) ionic strength.

According to Reimhult et al. [43], Richter et al. [44] and Michel et al. [45] who worked on the surface assembly of phospholipid vesicles the frequency evolution observed in the presented experiments is characteristic of vesicle adsorption without rupture. In principle, vesicle deposition followed by rupture would first lead to a frequency decrease and a subsequent increase and stabilisation of the signal. The increase in frequency is ascribed to the loss of water contained in the vesicles during their rupture (the opposite trend is observed for the dissipation). In this regard we should note that the frequency increase that we observe during the rinsing stage should be attributed to partial vesicle desorption from the multilayer. We can conclude from our data that the polymersomes remain intact during assembly, indicating major advantages over lipid vesicles that tend to rupture liberating encapsulated materials.

In Fig. 6 we observe the evolution of the adsorbed mass of a PBzMA-*b*-PDMAEMA/PSS multilayer. The regular frequency decrease after each adsorption step reveals the linear growth of the multilayer, thereby ruling out the presence of exponential or supralinear multilayer growth [46].

To explore the morphological features of the assembled interfacial architectures, $(PBzMA\text{-}b\text{-}PDMAEMA)_3/(PSS)_2$ films were prepared on top of silica quartz crystals, rinsed with distilled water, and imaged by AFM in tapping mode as described above. Fig. 7

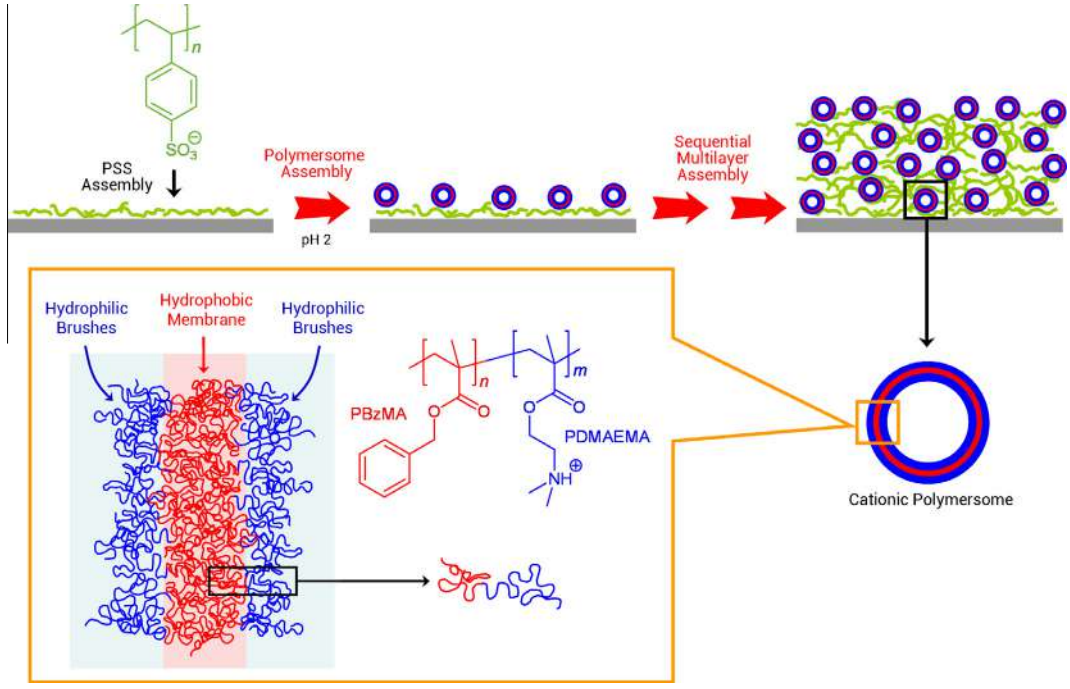

Fig. 4. Schematic of the film deposition process via sequential multilayer assembly using PSS and PBzMA-*b*-PDMAEMA polymersomes as building blocks. The figure also depicts a scheme of the polymersome membrane formed by self-assembled block copolymers as well as the chemical structures of the constituting building blocks.

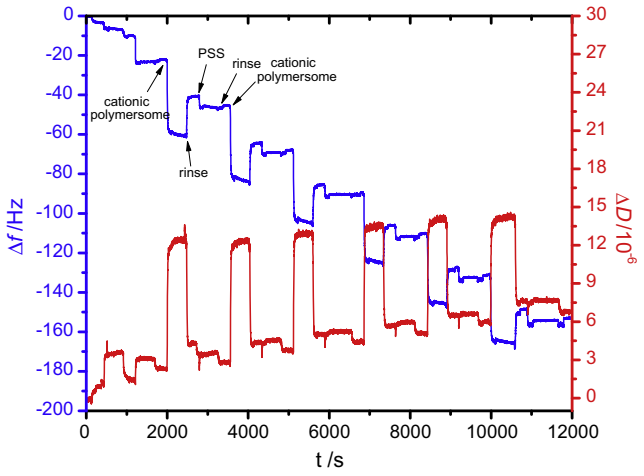

Fig. 5. In situ QCM-D monitoring of the LbL self-assembly of PBzMA-*b*-PDMAEMA polymersomes and PSS on silica coated quartz crystals. The blue trace represents frequency while the red trace represents dissipation. This QCM-D trace was obtained from 15 MHz harmonics (overtone $n = 3$). Three layers of PSS and polyethyleneimine (PEI) were initially assembled to provide a homogeneous PSS coating prior to the assembly of the first layer of polymersomes. (For interpretation of the references to colour in this figure legend, the reader is referred to the web version of this article.)

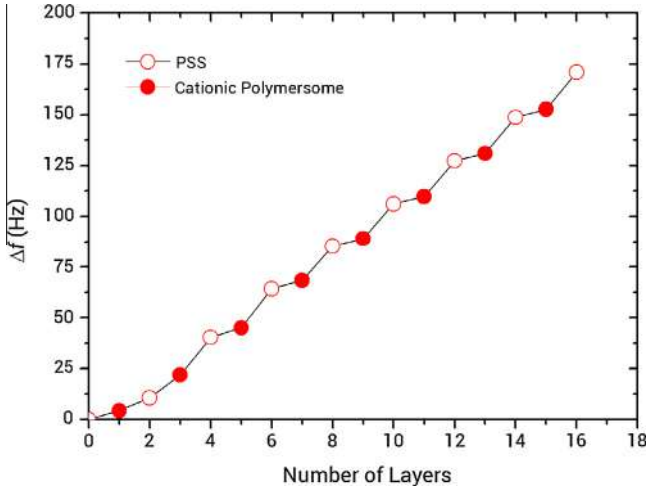

Fig. 6. QCM frequency shifts as a function of layer number for the alternate assembly of PBzMA-*b*-PDMAEMA vesicles and poly(styrene sulphonate) (PSS) on silica-coated QCM electrodes in 0.1 M KCl.

shows AFM images of planar LbL films, incorporating intact (PBzMA-*b*-PDMAEMA) polymersomes which, are evenly distributed over the entire surface. The cross-sectional profile indicates that the polymersomes are flattened upon loading onto the film, with a height ranging from 35 to 45 nm, and a diameter range of 270–290 nm which, corresponds to their size distribution measured by DLS (Fig. 1). AFM data corroborate that, in spite of a detectable deformation, polymersomes remain intact after surface assembly. Seminal work by Discher et al. [47,27] has demonstrated that polymersomes have highly flexible membranes that can tolerate deformation. The average diameter-to-height ratio of our electrostatically assembled polymersomes is 7.2 which is close to the value recently reported by Battaglia and his co-workers [31] for the immobilisation of biotinylated polymerosomes on streptavidin surfaces (diameter-to-height ratio = 7.75). This experimental observation is in agreement with the Seifert–Lipowsky model for the deformation of strongly adherent vesicles bound to planar surfaces [48].

Interestingly, the surface is covered with vesicles but one observes a large number of vacancies and inhomogeneities on the surface, meaning that the electrostatic assembly of polymersomes does not lead to the formation of a full compact monolayer. The multilayer growth mechanism has two important aspects to be taken into account: (a) the ability of an oppositely charged building block to be adsorbed in a second step on top of the first one and (b)

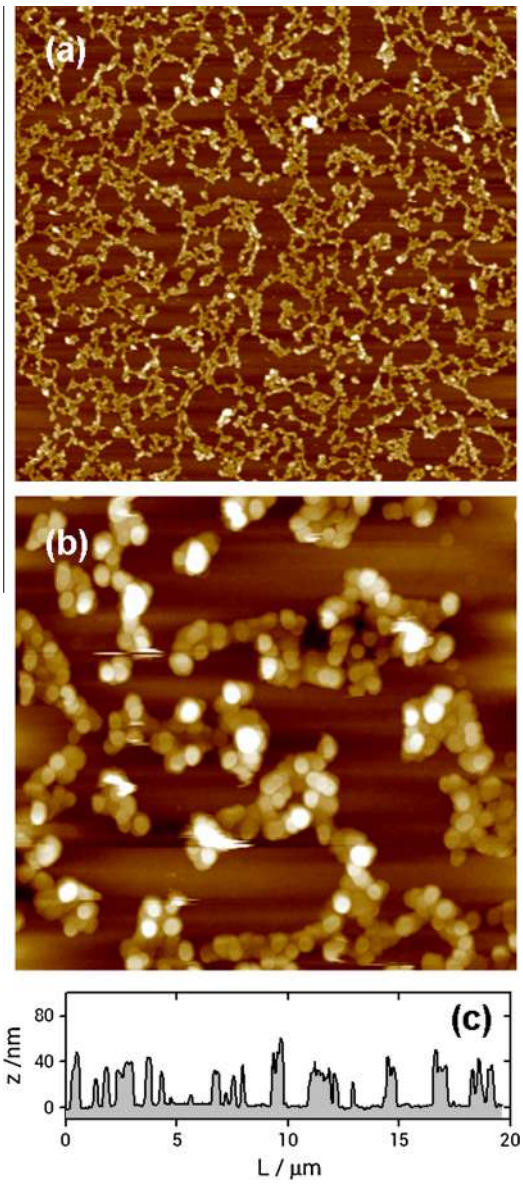

Fig. 7. AFM images of $(PBzMA\text{-}b\text{-}PDMAEMA)_3/(PSS)_2$ films: (a) 20 × 20 µm, (b) 5 × 5 µm. The figure also depicts the cross-sectional analysis resulting from AFM imaging (c).

repulsion between like-charged building blocks that ultimately leads to the self-regulation of the adsorption process and the formation of a "single" layer. It appears that in the case of polymersome assembly, charge reversal operates as expected in typical LbL systems without reaching full coverage by the polymersomes. In this regard we hypothesise that repulsive electrostatic and steric interactions between highly charged bulky vesicles play a dominant role and restrict the formation of compact monolayers. However, the presence of a charged PDMAEMA block on the outer surface of the polymersomes is sufficient to promote efficient charge reversal under low coverage conditions.

Using a strategy similar to that implemented on planar substrates, a polymersome/polyelectrolyte multilayer was deposited on spherical silica particles. Fig. 8 shows the variation in the ζ potential of silica particles coated with polymersomes and PSS as a function of the number of layers. The initially negative ζ potential of the silica surface becomes positive after adsorption of the cationic PBzMA-*b*-PDMAEMA vesicles. The subsequent addition of

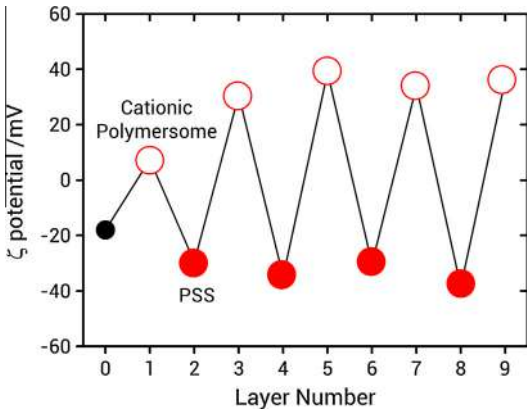

Fig. 8. ζ Potential as a function of layer number for the polymersome/polyelectrolyte-coated silica. The error bars are smaller than the symbol size.

PSS led to surface charge reversal, producing a negative ζ potential. Each successive deposition results in complete charge reversal, indicating a successful coating by the oppositely charged building blocks.

To confirm polymersome incorporation into multilayered structures on silica colloid surfaces, we performed fluorescence experiments using rhodamine B-loaded polymersomes. CLSM performed on the silica core–multilayered shell particles indicated the incorporation of the polymersomes within multilayered shells comprising sequential (PBzMA-*b*-PDMAEMA)/PSS assemblies (Fig. 9a and b) [49]. In our case, additional CLSM experiments showed that the assembly process taking place on the colloidal surface promotes neither polymersome rupture nor loss of the dye entrapped from the multilayered shells.

CLSM imaging of the silica particles coated with the (PBzMA-b-PDMAEMA) polymersomes with encapsulated rhodamine B showed highly fluorescent particles (Fig. 9a and b). The size of the particles after sequential LbL assembly was significantly larger than bare silica particles, which had a diameter close to 500 nm. Polymersome-coated particles showed diameters in the 3–5 µm range, the diameter of the polymersomes is 275 nm. For example, deposition of four polymersome/polyelectrolyte bilayers onto bare silica particles resulted in an increase of the mean particle diameter from 500 nm to 3.15 µm, as corroborated by SEM imaging (Fig. 9c and d).

Close inspection of the morphology of the surface-modified multilayer-coated particles using TEM revealed the presence of polymersomes in different interfacial configurations. Most of the samples showed a clear flattening or spreading of the polymersomes homogeneously distributed on the particle surface. We hypothesise that this structural reorganisation may also lead to interpenetration of subsequent layers, and also to film compression. On the other hand, some samples revealed the presence of intact polymersomes on the outermost layer of the multilayer coating leading to an increase in the apparent roughness of the polymersome-coated silica particles. The striking difference with the planar surface coating may come from the difference in the assembly procedures. In the case of colloidal particles, the assembly of consecutive layers is performed using centrifugation steps to remove an excess of polyelectrolyte and polymersomes after each deposition. During centrifugation particles and polymersomes become densily packed and this can lead to the reorganisation of the layers and packing of the polymersomes and polyelectrolytes resulting in structures with thicknesses that correspond to a dense polymersome layer. This is not possible in the case of planar surfaces where substrates are sequentially immersed in polymersome, PSS and rinsing solutions during LbL assembly.

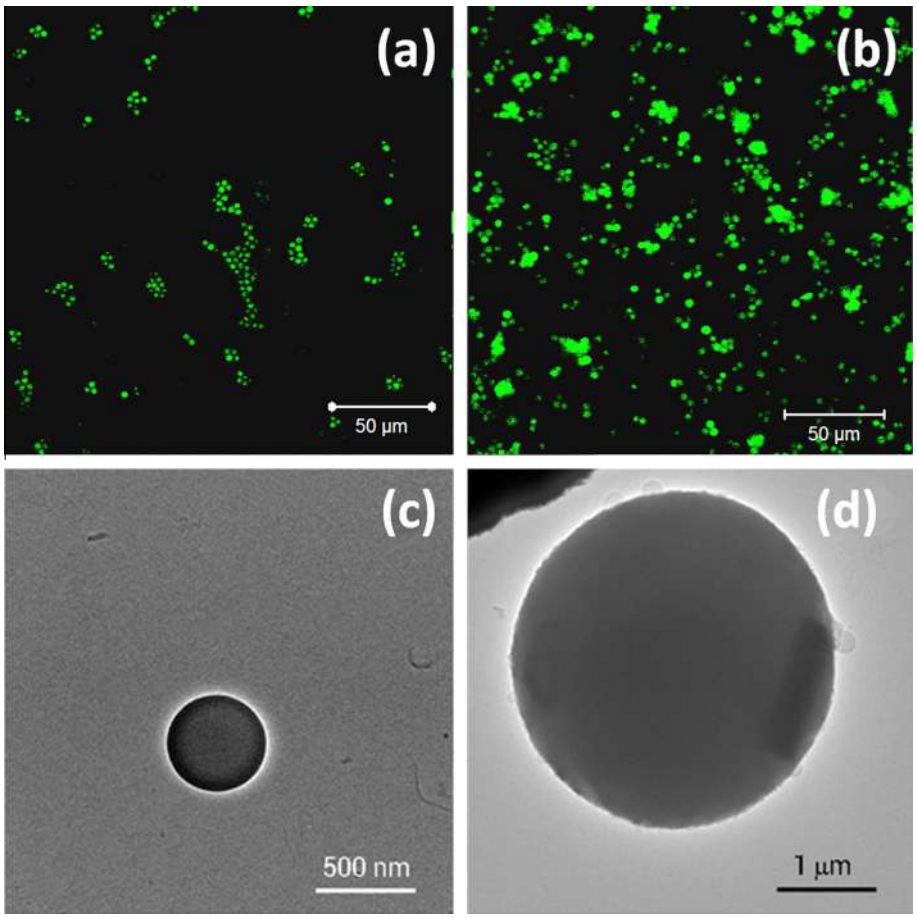

Fig. 9. (a) CLSM image of silica colloids with 1 multilayer. (b) CLSM image of silica colloids with 4 multilayers. (c) TEM image of bare silica colloid. (d) TEM image of silica colloid coated with $(PBzMA\text{-}b\text{-}PDMAEMA)_4/(PSS)_4$ multilayers. Samples were stained with ammonium molibdate.

The subject of vesicle adhesion on solid surfaces has been very active in recent years, particularly in the case of lipid vesicles [50,51]. At present it is widely accepted that adhering vesicles can exhibit a large variety of different shapes provided that adhesion can change the topology since it can induce structural reorganisation of the membrane constituents [52,53]. For instance, in most cases vesicles undergo a nontrivial adhesion transition from a free to a bound state. This transition is governed by the balance between the overall bending and adhesion energies, and occurs even in the absence of shape fluctuations. According to the model proposed by Seifert and Lipowsky for lipid vesicles in the presence of an attractive surface, a vesicle can undergo shape transformations between a free and a bound state, and between two different bound states. The local stability of the bound vesicle determines to a great extent the presence of these various (metastable) states. Our TEM characterisation (Fig. 10) revealed an analogous scenario for the electrostatic assembly of charged polymersomes on a polyelectrolyte layer. To the best of our knowledge this is the first detailed visualisation of different bound states of intact polymersomes coexisting on a solid surface.

Regardless of the morphological aspects of the polymersome layer, we observed that subsequent adsorption of PSS forms a very uniform layer that covers the entire colloidal particle. Fig. 11(left panel) shows a SEM image of a PSS-capped colloidal particle modified with a polymersome/polyelectrolyte multilayer. It can be clearly seen that polymersomes buried underneath the PSS layer

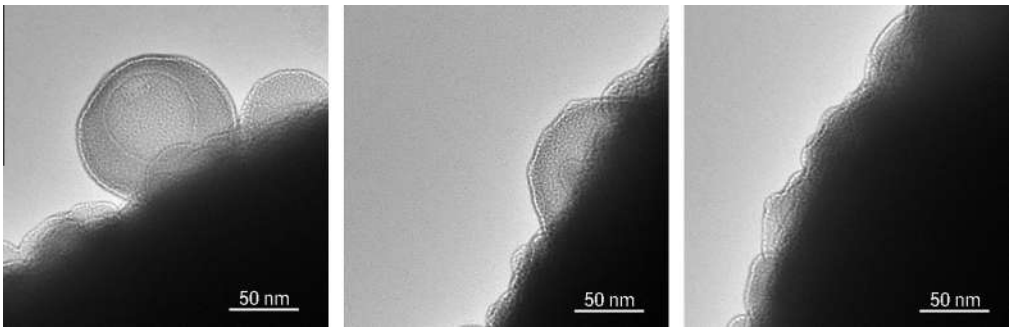

Fig. 10. TEM images of polymersome-coated silica particles showing that adhering vesicles exhibit a variety of different shapes. Scale bars = 50 nm.

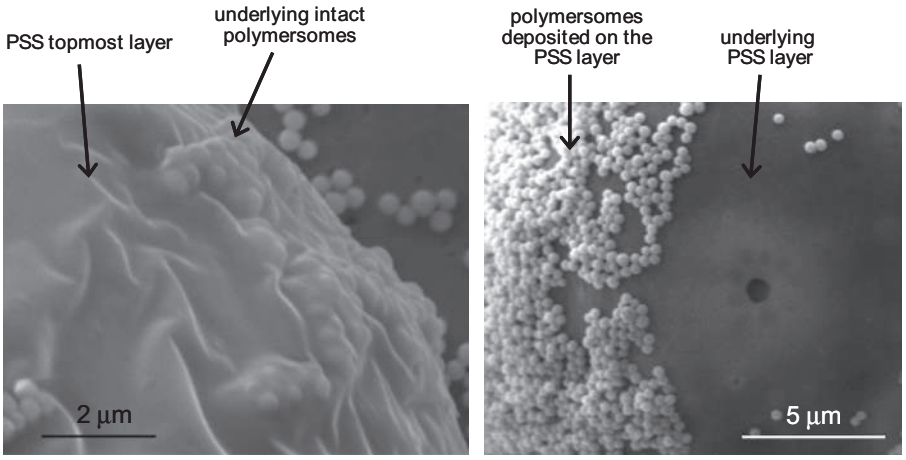

Fig. 11. (Left panel) SEM micrograph of a silica colloid modified with a (PBzMA-*b*-PDMAEMA)$_2$/PSS$_3$ multilayer. (Right panel) SEM micrograph of a colloidal silica particle modified with a polymersome/PSS assembly. The image shows the adsorption of cationic vesicles on the anionic polyelectrolyte.

remain intact after the polyelectrolyte adsorption. In the case of polymersomes as capping layers Fig. 11(right panel) we can observe a partial removal of the polymersomes probably due to the drying process. Nevertheless, SEM imaging allows us to appreciate how smooth the surface of the multilayer assembly becomes after PSS adsorption.

4. Conclusions

Successful formation of multilayer films on a planar silica substrate by alternate self-assembly of cationic (PBzMA-*b*-PDMAEMA) polymersomes and PSS has been presented on the basis of QCM-D and AFM data. We have shown that polymeric vesicles can be assembled in polyelectrolyte multilayers without rupturing. In situ LbL deposition of each successive layer results in (i) complete and reproducible charge reversal of the adsorbed multilayer film, (ii) a monotonic linear increase in the cumulative adsorbed amount of polymersome and PSS constituting the film, (iii) formation of the island-like surface aggregates (even for 4 deposited layers of polymersomes) due to strong electrosteric repulsion between charged vesicles. On the basis of the QCM-D data, a structural transformation of the adsorbed building blocks is suggested to occur over sequential assembly of (PBzMA-*b*-PDMAEMA) polymersomes and PSS. The assembly on top of colloidal particles was studied by ζ potential . CLSM, TEM, and SEM further corroborated the formation of the assemblies on top of the silica. For 4 deposited layers of polymersomes on top of the silica particles the total size of the particles increases from 500 nm to more than 3 μm. This size increase is in agreement with the deposition of densely packed layers of polymersomes. The differences in the layer structure for planar and colloidal particles under the same assembly conditions can be explained by the high density of polymersomes around the particles during centrifugation that triggers a dense packing and full coverage of the surface of the colloidal particles. Based on the results obtained in the present study using a number of different experimental techniques, the approach shown here could provide a basis for designing hierarchical multilayered assemblies with multiple storage functions, taking full advantage of the hollow nanoscale polymersomes.

Acknowledgments

This work was financially supported by the Marie Curie project "*Transport Studies on Polymer Based Nanodevices and Assemblies for Delivery and Sensing*" (TRASNADE) (Grant ref: 247656). M.E.C. gratefully acknowledges a doctoral fellowship from CONICET. O.A. is a CONICET fellow and acknowledges financial support from the Alexander von Humboldt Stiftung (Germany), the Max Planck Society (Germany), ANPCyT-Argentina (PICT-PRH 163/08, PICT-2010-2554) and the Austrian Institute of Technology GmbH (AIT–CONICET Partner Group: "*Exploratory Research for Advanced Technologies in Supramolecular Materials Science*" – Exp. 4947/11, Res. No. 3911, 28-12-2011). S.M. acknowledges support from the Spanish Ministry of Science and Innovation (MAT2010-18995).

Appendix A. Supplementary material

Supplementary data associated with this article can be found, in the online version, at http://dx.doi.org/10.1016/j.jcis.2014.01.038.

References

[1] G. Decher, in: G. Decher, J.B. Schlenoff (Eds.), Multilayer Thin Films, Wiley-VCH, Wienheim, 2002, pp. 1–46 (Chapter 1).
[2] K. Ariga, J.P. Hill, Q. Ji, Phys. Chem. Chem. Phys. 9 (2007) 2319–2340.
[3] M.-K. Park, R.C. Advincula, in: W. Knoll, R.C. Advincula (Eds.), Functional Polymer Films. Vol. 1: Preparation and Patterning, VCH-Wiley, Weinheim, 2011, pp. 73–112 (Chapter 3).
[4] P. Bertrand, A.M. Jonas, A. Laschewsky, R. Legras, Macromol. Rapid Commun. 21 (2000) 319–348.
[5] (a) E.V. Skorb, D.V. Andreeva, Polym. Chem. 4 (2013) 4834–4845;
(b) K. Ariga, Q. Ji, J.P. Hill, Y. Bando, M. Aono, NPG Asia Mater. 4 (2012) e17.
[6] P.T. Hammond, Adv. Mater. 16 (2004) 1271–1293.
[7] E. Donath, S. Moya, B. Neu, G.B. Sukhorukov, R. Georgieva, A. Voigt, H. Bäumler, H. Kiesewetter, H. Möhwald, Chem. Eur. J. 8 (2002) 5481–5485.
[8] E. Donath, G.B. Sukhorukov, F. Caruso, S.A. Davis, H. Möhwald, Angew. Chem. Int. Ed. 37 (1998) 2202–2205.
[9] D.M. Sullivan, M.L. Bruening, J. Am. Chem. Soc. 123 (2001) 11805–11806.
[10] D. Pallarola, C. von Bildering, L.I. Pietrasanta, N. Queralto, W.Knoll.F. Battaglini, O. Azzaroni, Phys. Chem. Chem. Phys. 14 (2012) 11027–11039.
[11] O. Azzaroni, K.H.A. Lau, Soft Matter 7 (2011) 8709–8724.
[12] M. Ali, B. Yameen, J. Cervera, P. Ramírez, R. Neumann, W. Ensinger, W. Knoll, O. Azzaroni, J. Am. Chem. Soc. 132 (2010) 8338–8348.
[13] G. Decher, Science 277 (1997) 1232–1237.
[14] F. Caruso, H. Möhwald, J. Am. Chem. Soc. 121 (1999) 6039.
[15] (a) V.V. Tsukruk, F. Rinderspacher, V.N. Bliznyuk, Langmuir 13 (1999) 2171;
(b) A.J. Khopade, F. Caruso, Nano Lett. 2 (2002) 415.
[16] S. Moya, E. Donath, G.B. Sukhorukov, M. Auch, H. Bäumler, H. Lichtenfeld, H. Möhwald, Macromolecules 33 (2000) 4538–4544.
[17] (a) F. Caruso, M. Spasova, Adv. Mater. 13 (2001) 1090;
(b) R.A. Caruso, A. Susha, F. Caruso, Chem. Mater. 13 (2001) 400;
(c) T. Sennerfors, G. Bogdanovic, F. Tiberg, Langmuir 18 (2002) 6410.
[18] (a) N. Ma, H. Zhang, B. Song, Z. Wang, X. Zhang, Chem. Mater. 17 (2005) 5065;
(b) B. Qi, X. Tong, Y. Zhao, Macromolecules 39 (2006) 5714;
(c) J. Cho, J. Hong, K. Char, F. Caruso, J. Am. Chem. Soc. 128 (2006) 9935;
(d) S. Biggs, K. Sakai, T. Addison, A. Schmid, S.P. Armes, M. Vamvakaki, V. Bütün, G.B. Webber, Adv. Mater. 19 (2007) 247.
[19] (a) Z. Zhu, S.A. Sukhishvili, J. Mater. Chem. 22 (2012) 7667–7671;
(b) L. Xu, Z. Zhu, S.A. Sukhishvili, Langmuir 27 (2011) 409–415;

(c) J. Choi, M.F. Rubner, J. Macromol. Sci. Pure Appl. Chem. 38A (2001) 1191–1206.
[20] (a) M. Michel, D. Vautier, J.C. Voegel, P. Schaaf, V. Ball, Langmuir 20 (2004) 4835;
(b) M. Michel, A. Izquierdo, G. Decher, J.C. Voegel, P. Schaaf, V. Ball, Langmuir 21 (2005) 7854.
[21] J. Li, Q. He, X. Yan, Molecular Assembly of Biomimetic Systems, VCH-Wiley, Weinheim, 2011 (Chapter 2).
[22] X. Shia, M. Shen, H. Möhwald, Prog. Polym. Sci. 29 (2004) 987–1019.
[23] N. Ma, H.Y. Zhang, B. Song, Z.Q. Wang, X. Zhang, Chem. Mater. 17 (2005) 5065.
[24] K. Katagiri, R. Hamasaki, K. Ariga, J. Kiguchi, Langmuir 18 (2002) 6709–6711.
[25] A. Katagiri, R. Hamasaki, K. Ariga, J. Kiguchi, J. Am. Chem. Soc. 124 (2002) 7892–7893.
[26] H. Lomas, A.P.R. Johnston, G.K. Such, Z. Zhu, K. Liang, M.P. van Koeverden, S. Alongkornchotikul, F. Caruso, Small 7 (2011) 2109–2119.
[27] D.E. Discher, F. Ahmed, Annu. Rev. Biomed. Eng. 8 (2006) 323–341.
[28] K. Kita-Tokarczyk, J. Grumelard, T. Haefele, W. Meier, Polymer 46 (2005) 3540–3563.
[29] C. LoPresti, H. Lomas, M. Massignani, T. Smart, G. Battaglia, J. Mater. Chem. 19 (2009) 3576–3590.
[30] B.M. Discher, Y.-Y. Won, D.S. Ege, J.C.-M. Lee, F.S. Bates, D.E. Discher, D.A. Hammer, Science 284 (1999) 1143.
[31] G. Battaglia, C. LoPresti, M. Massignani, N.J. Warren, J. Madsen, S. Forster, C. Vasilev, J.K. Hobbs, S.P. Armes, S. Chirasatitsin, A.J. Engler, Small 7 (2011) 2010–2015.
[32] V. Malinova, S. Belegrinou, D. de Bruyn Ouboter, W.P. Meier, Adv. Polym. Sci. 224 (2010) 113–165.
[33] I.B. Dicker, G.M. Cohen, W.B. Farnham, W.R. Hertler, E.D. Laganis, D.Y. Sogah, Macromolecules 23 (1990) 4034–4041.
[34] O.W. Webster, J. Polym. Sci. A Polym. Chem. 38 (2000) 2855–2860.
[35] O.W. Webster, Adv. Polym. Sci. 167 (2004) 1–34.
[36] V. Bütün, M. Vamvakaki, N.C. Billingham, S.P. Armes, Polymer 41 (2000) 3173–3182.
[37] G.B. Sukhorukov, E. Donath, H. Lichtenfeld, E. Knippel, M. Knippel, A. Budde, H. Möhwald, Colloids Surf. A: Physicochem. Eng. Aspects 137 (1998) 253–266.
[38] J. Du, R.K. O'Reilly, Soft Matter 5 (2009) 3544–3561.
[39] F. Rehfeldt, R. Steitz, S.P. Armes, R. von Klitzing, A.P. Gast, M. Tanaka, J. Phys. Chem. B 110 (2006) 9171.
[40] S. Moya, O. Azzaroni, T. Farhan, V.L. Osborne, W.T.S. Huck, Angew. Chem. Int. Ed. 44 (2005) 4578–4581.
[41] S.E. Moya, O. Azzaroni, T. Kelby, E. Donath, W.T.S. Huck, J. Phys. Chem. B 111 (2007) 7034–7040.
[42] I. Llarena, J.J. Iturri Ramos, E. Donath, S.E. Moya, Macromol. Rapid Commun. 31 (2010) 526–531.
[43] E. Reimhult, F. Höök, B. Kasemo, Langmuir 19 (2003) 1681–1691.
[44] R. Richter, A. Mukhopadhyay, A. Brisson, Biophys. J. 85 (2003) 3035–3047.
[45] M. Michel, D. Vautier, J.-C. Voegel, P. Schaaf, V. Ball, Langmuir 20 (2004) 4835–4839.
[46] M. Michel, A. Izquierdo, G. Decher, J.-C. Voegel, P. Schaaf, V. Ball, Langmuir 21 (2005) 7854–7859.
[47] D.E. Discher, A. Eisenberg, Science 297 (2002) 967–973.
[48] U. Seifert, R. Lipowsky, Phys. Rev. A 42 (1990) 4768–4771.
[49] S. Biggs, K. Sakai, T. Addison, A. Schmid, S.P. Armes, M. Vamvakaki, V. Bütün, G. Webber, Adv. Mater. 19 (2007) 247–250.
[50] U. Seifert, K. Berndl, R. Lipowsky, Phys. Rev. A 44 (1991) 1182–1202.
[51] M.J. Blount, M.J. Miksis, S.H. Davis, Eng. Sci. 469 (2013) 20120729.
[52] K. Dimitrievski, Langmuir 26 (2010) 3008–3011.
[53] C. Lv, Y. Yin, J. Yin, Colloids Surf. B: Biointerfaces 74 (2009) 380–388.